American Mineralogist, Volume 75, pages 1249–1252, 1990

Rietveld refinement of the high-pressure polymorph of Mn_3O_4

CHARLES R. ROSS II, DAVID C. RUBIE, ELEONORA PARIS*
Bayerisches Geoinstitut, Universität Bayreuth, Postfach 10 12 51, 8580 Bayreuth, Germany

ABSTRACT

The structure of a high-pressure polymorph of Mn_3O_4 has been refined using the Rietveld technique. The structure is confirmed to be isostructural with $CaMn_2O_4$ (marokite), but with significant changes caused by the substitution of divalent Mn for Ca in the large triangular channels.

INTRODUCTION

Under ambient conditions, Mn_3O_4 adopts a distorted spinel structure and has the mineral name hausmannite (Jarosch, 1987). At high pressures, this structure becomes unstable, and a new polymorph is formed (Reid and Ringwood, 1969). Although this high-pressure polymorph has been reported to be isostructural with the mineral marokite ($CaMn_2O_4$, Lepicard and Protas, 1966), a complete refinement of this structure has never been performed. The $CaMn_2O_4$ structure is itself a distortion of the $CaTi_2O_4$ structure; this structure, or a topological equivalent, is adopted by several compositions, including $NaAlSiO_4$ at high pressure (Muller and Roy, 1974; Liu and Bassett, 1986). For convenience, the high-pressure polymorph will be here identified as Mn_3O_4 II and the low-pressure form identified as Mn_3O_4 I.

Previously reported identification of Mn_3O_4 II has been as a product of high-pressure phase transformation (Reid and Ringwood, 1969; Paris et al., in preparation). The ability of the multianvil high-pressure apparatus to achieve pressures of 10–20 GPa simultaneously with temperatures in excess of 1200 °C has been utilized to synthesize relatively large quantities of Mn_3O_4 II for characterization in this study.

EXPERIMENTAL DETAILS

The sample of Mn_3O_4 II used for the structure refinement in this study was synthesized in a 1200-ton uniaxial split sphere apparatus (Ito et al., 1984) at the Bayerisches Geoinstitut at 10.5 GPa and 1000 °C for 1 h. The truncation edge length of the inner tungsten carbide anvils was 11 mm. The sample assembly consisted of a MgO octahedron, with an edge length of 18 mm, containing a cylindrical graphite heater that was surrounded by a sleeve of ZrO_2 for thermal insulation. The starting material was powdered reagent-grade Mn_3O_4 I, which was sealed in a Pt capsule. Temperature was monitored using a Pt-Pt, 10% Rh thermocouple and pressure was calibrated against the hydraulic oil pressure using transitions in Bi at room temperature and the coesite-stishovite transition at 1000 °C.

Samples of Mn_3O_4 II have also been synthesized at 15 GPa in the uniaxial split-sphere apparatus. At this pressure, Mn_3O_4 II is stable at temperatures in the range 25 °C to >1200 °C. The transformation of Mn_3O_4 I to Mn_3O_4 II is rapid over the entire temperature range, requiring less than 1 h when under pressure; however, at room temperature the crystallinity of the Mn_3O_4 II that forms is poor.

An X-ray powder diffraction pattern of the sample synthesized at 10.5 GPa and 1000 °C showed that it consisted of well-crystallized Mn_3O_4 II. Although no Mn_3O_4 I was detected, small but significant quantities of α-Mn_2O_3 were present. Small quantities of unidentified impurities were also detected in samples synthesized at 15 GPa and probably originated by limited reaction between the sample and the pressure medium.

The sample was prepared by removing the sintered pellet of Mn_3O_4 II from the experimental assembly and grinding it in an agate mortar to an average grain size of approximately 15 μm (although the average crystallite size appeared somewhat smaller). This powder was then mounted on a thin plastic foil with a solution of polyvinylic alcohol and distilled H_2O. When dry, the sample was covered with a second foil (to prevent contamination) and mounted in a circular sample holder. This holder is inserted in the powder diffractometer in such a way that the sample can be rotated about an axis normal to the plane of the sample; this axis is coplanar with the incident and diffracted X-ray beams, and rotation about it improves counting statistics (particularly with a small sample) by bringing a larger number of crystallites into the diffraction condition.

Data for Rietveld refinement were measured in the transmission mode using a Stoe STADIP automated powder diffractometer. A position-sensitive detector of 7.4° width and 0.02° data interval was used; as this diffractometer has a primary beam (but no diffracted beam) monochromator, Mo$K\alpha$ radiation was used to eliminate fluorescence. Variations in sensitivity across the detector were minimized by taking 0.2° steps between data measurements; i.e., each position in 2θ was measured at 37

* Permanent address: Dipartimento di Scienze della Terra, Universitá di Camerino, 62032 Camerino (MC), Italy.

0003–004X/90/1112–1249$02.00

(= 7.4°/0.2°) evenly spaced positions on the detector. Eleven replicate patterns from 5 to 50° 2θ were obtained (to minimize the effect of instrumental drift as well as short-period fluctuations) and then summed; each data point represents 4070 s of counting time.

Structure refinement

To minimize the influence of the presence of α-Mn_2O_3, five regions of the X-ray data were not used in the refinement, i.e., 10.0–11.0°, 14.5–15.5°, 16.8–17.8°, 24.1–25.1°, and 28.5–29.5° 2θ. These regions are centered on the five largest peaks of the α-Mn_2O_3 pattern, as indicated in JCPDS card 24-508, and extend for approximately three peak half-widths on either side. No other peaks in the α-Mn_2O_3 pattern are reported to have $I/I_0 > 10\%$. The removal of these regions was necessary for unambiguous refinement of the Mn_3O_4 II structure, but the removal of ca. 10% of the data (including several prominent peaks) inevitably degraded the quality of the refinement. This was evident when comparing the results of this refinement with results of trial refinements (using all data) of Mn_3O_4 II which was contaminated with small amounts of an unknown phase. These refinements converged to significantly smaller R factors than the present refinement, but as the influence of the contaminant could not be gauged, these refinements were unsatisfactory.

The structure was refined in space group *Pmab* (a non-standard setting of *Pbcm,* but the one used by Lepicard and Protas, 1966) using the program DBW (Wiles and Young, 1981), beginning with the structure parameters of $CaMn_2O_4$ of Lepicard and Protas (1966). On the basis of experience fitting standard materials (e.g., NBS Standard Reference Material 600 for 2θ line profiles), a pseudo-Voigt profile with 2θ-independent Gaussian fraction was used; the Gaussian fraction, peak asymmetry, and U, V, and W half-width parameters (Young and Wiles, 1982) were refined. Peak base was taken to be 10 × FWHM. Four background parameters were refined; the background was assumed to have the form

$$I_{bkg}(2\theta_i) = B_0 + B_1\Delta_i + B_2\Delta_i^2 + B_3\Delta_i^3$$

where B_i is the ith background parameter and

$$\Delta_i = \frac{2\theta_i}{90} - 1.$$

The use of a primary-beam monochromator [Ge(111), singly curved] reduces the presence of the Mo$K\alpha_2$ component in the X-ray beam. After some trial fitting of the pattern using different values of $I(K\alpha_2)/I(K\alpha_1)$, it was found that the best results were obtained when a value of zero was used, and thus $\lambda = 0.7093$ Å. The monochromator correction (Azároff, 1955) was set at its theoretical value. For this sample, $I_0/I = 2.95$, but no absorption correction was applied; the limited range in 2θ minimized the effect of absorption on the refinement.

Initially, an overall temperature factor with the ratio $B_{Mn}/B_O = 0.8/1$ was refined, following Post and Bish (1988) for the Rietveld refinement of todorokite, but this model resulted in a negative overall temperature factor of $-0.49(3)$ Å^2. As a negative temperature factor has no physical meaning, various alterations in the model were tested, ultimately resulting in the refinement of three temperature factors: one for each Mn and one for all O atoms. This model shows positive temperature factors, but curiously, the O temperature factor is the smallest of the three.

For the last several refinement cycles, all parameters were refined simultaneously. The refinement converged to R_P of 3.45 and R_{WP} of 4.40. Other refinement statistics are reported in Table 1, and the refined pattern and structural parameters are reported in Table 2. Figure 1 compares the observed intensities, calculated intensities, and the difference in observed and calculated intensities, as well as giving the calculated peak positions for the refined structure. Correlations among the structure parameters tended to be small, exceptions being among the unit-cell parameters (0.56–0.59) and between the x-coordinates of the two Mn atoms (0.59).

There are two aspects of the refinement that are of concern. First, the temperature factors of the Mn atoms are significantly larger than those for O. This is unlikely to be due to thermal vibration alone, as Mn is ca. 3.4 times more massive than O. A possible explanation is that the Mn atoms are disordered on their respective sites, and that the large temperature factor is modeling two (or more) atomic positions. As a calculation of bond length to bond strength (Brown and Altermatt, 1985) reveals that the

Table 1. Final refinement statistics

R_P	3.45
R_{WP}	4.40
R_{exp}	4.89
S (goodness of fit)	0.90
Derived R_{Bragg}	4.81
Weighted Durbin-Watson D	0.79
Total refined parameters	28
Degrees of freedom (observations-parameters)	1967

Table 2. Pattern and structural parameters

Asymmetry parameter:		0.12(4)		
FWHM (at 30°2θ):		0.125°		
Gaussian fraction:		0.57(1)		
Half-width parameters:	U	0.11(2)		
	V	−0.042(8)		
	W	0.020(1)		

$$FWHM^2 = U\tan^2\theta + V\tan\theta + W$$

Cell parameters:

a	9.5564(3) Å
b	9.7996(3) Å
c	3.0240(1) Å

Structural parameters:

Atom	x	y	z	B
Mn^{2+}	¾	0.1461(1)	0.6845(7)	0.55(4)
Mn^{3+}	0.0696(1)	0.1147(1)	0.2034(5)	0.25(3)
O(I)	0	¼	0.6204(18)	0.18(7)
O(II)	¼	0.1999(6)	0.1899(20)	*
O(III)	0.1112(4)	0.9694(5)	0.7956(15)	*

* B is identical for all O atoms.

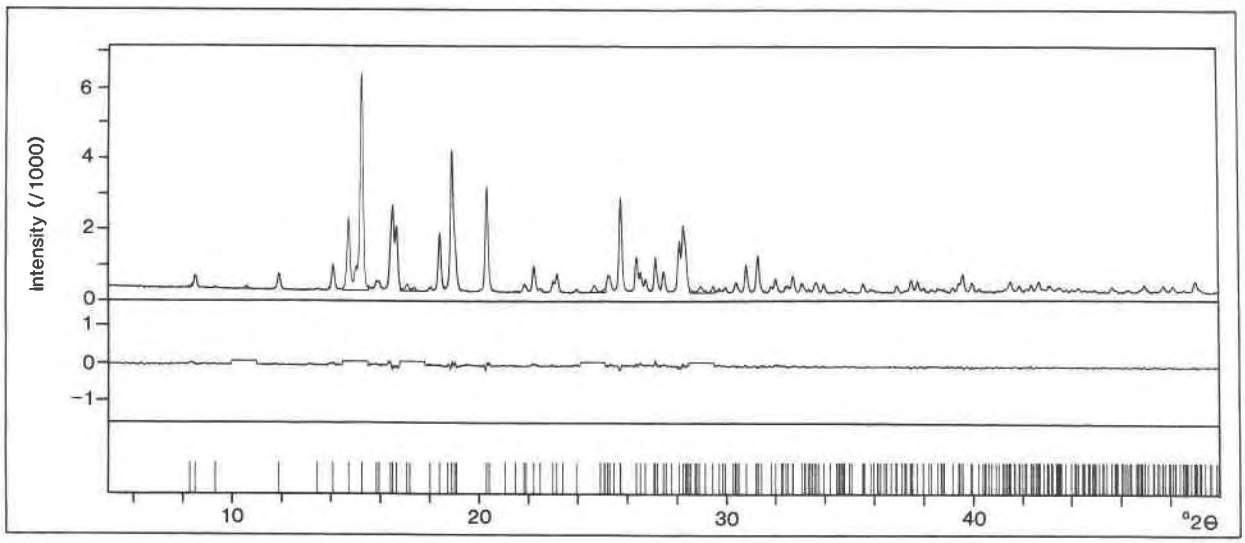

Fig. 1. X-ray pattern of Mn_3O_4 II. Upper section is observed and calculated intensity. Center section corresponds to the difference in observed and calculated intensity (to same scale). Lower section indicates the location of individual Bragg reflections. In the difference plot (center), the regions that were excluded from the refinement are slightly displaced for clarity.

two Mn atoms are nearly perfectly charge balanced (1.997 and 3.007 e^- respectively), it seems unlikely that any significant amount of disorder exists. The most probable explanation is that the temperature parameters are in error: temperature factors tend to include accumulated errors in refinement, and thus are among the least reliable parameters.

The second factor of concern is that the Durbin-Watson (DW) statistic is so small. This statistic measures the correlation between adjacent least-squares residuals (i.e., serial correlation, Flack and Vincent, 1980; Hill and Flack, 1987). Possible sources of correlation suggested by Hill and Flack (1987) include (1) short-term fluctuations in the X-ray beam intensity, (2) variations in integrated peak intensities due to preferred orientation, (3) deficiencies in the structural model, (4) errors or asymmetry in the peak shape and (5) variations in peak position and width due to crystallite size and strain effects. In addition, (6) variations in sensitivity at different positions across the detector must be considered as a possible source of correlation.

The averaging of 11 replicate patterns should minimize the effect of fluctuations in the X-ray beam intensity (1). Inspection of the pattern for the difference in observed and calculated intensities (Fig. 1, center) shows that although some correlation exists between observed diffraction peaks and residual intensity, it is neither strong nor systematic. Therefore, although model errors such as (2)–(5) above cannot be eliminated, it seems unlikely that they alone are responsible for the low DW statistic. Finally, the data were analyzed to evaluate the influence of nonuniformity of the detector. This should appear as a systematic fluctuation with a period (due to the collection interval) of 0.2°. The analysis revealed only weak systematic fluctuations, but detailed inspection of the difference intensity revealed irregular, long-wavelength fluctuations of amplitude too small to be readily detected in Figure 1. The source of this fluctuation is unknown, although it is possibly caused by errors in background fitting.

In an attempt to improve the DW statistic, trial refinements using different peak profiles, as well as different numbers of background parameters, were performed. No alternate choice of peak profile improved the DW statistic. Refining one less (3) background parameter resulted in a significant increase in the R factor, whereas high correlations among the background parameters made fitting of an additional parameter impossible. Finally, the low value of the goodness-of-fit parameter (S, Table 1), suggests that the refinement is nearly optimized, and so no significant change in the DW statistic may be expected with any alteration in the model.

The DW statistic is crucial in that it reflects the reliability of the refinement. It has been shown (Hill and Flack, 1987) that in some cases there is a strong correlation between the precision (but not the accuracy) of values of structural parameters and the DW statistic. Thus in these cases the DW statistic is a measure of the reliability of the estimated standard deviations. As the source of the anomalous DW statistic is unknown, application to the present work is problematic, but suggests that the reported estimated standard deviations are unrealistically small.

Discussion

The structure of Mn_3O_4 II is (as hypothesized) isostructural with $CaMn_2O_4$ (marokite), but with significant changes caused by the substitution of Mn^{2+} for Ca^{2+}. The structure of Mn_3O_4 II is dominated by edge-sharing strips

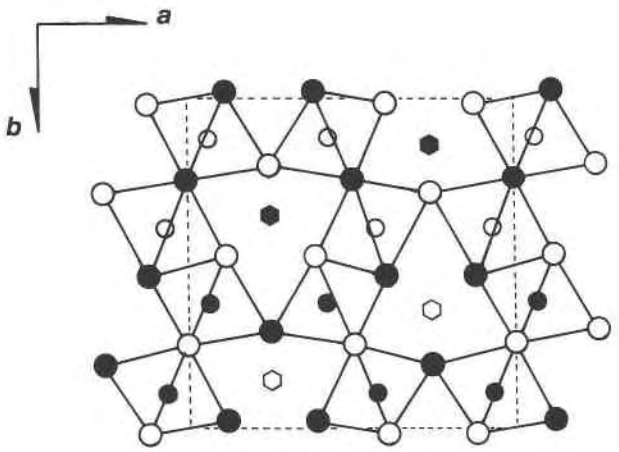

Fig. 2. Crystal structure of Mn_3O_4 II, projected along c axis. Large circles indicate O atoms, small circles Mn^{3+}, and hexagons Mn^{2+}. Open circles are at $z \simeq 0.2$, open hexagons are at $z \simeq 0.3$, filled circles at $z \simeq 0.8$, filled hexagons at $z \simeq 0.7$.

of octahedral Mn^{3+} running parallel to the c axis (Fig. 2). These strips are two octahedra wide, and are linked into a herringbone pattern, and thus enclose triangular channels within which Mn^{2+} is found in highly irregular coordination. The coordinations of Mn^{3+} and Mn^{2+} are summarized in Table 3.

The Mn^{3+} site is an axially distorted octahedral site; the two long apical bonds average 2.313 Å and the four short equatorial bonds average 1.926 Å in length. Quadratic elongation values (Hazen and Finger, 1982) imply that this site is slightly less distorted than the equivalent site in $CaMn_2O_4$; however the quadratic elongation is slightly larger in $CaMn_2O_4$. In addition, the Mn^{3+} and Mn^{2+} sites are smaller (approximately 5% and 14%, respectively) in Mn_3O_4 II than in $CaMn_2O_4$ (Table 3) because of the substitution of the smaller Mn^{2+} for Ca^{2+}.

The structure of Mn_3O_4 II is in many ways reminiscent of that of hollandite (Post et al., 1982), the primary difference being that the channels in hollandite are square whereas in Mn_3O_4 II they are triangular. As the sides of the channels in both materials are defined by double octahedral strips, the channels in Mn_3O_4 II are substantially smaller than those in hollandite. As Mn_3O_4 II is only stable at high pressures, whereas $CaMn_2O_3$ may be synthesized at high temperature (Lepicard and Protas, 1966), it appears that the Mn^{3+} ion is slightly too small for the channels, and that species with ionic radii on the order of 1 Å (e.g., Cd) would be favored by this structure.

Table 3. Metal-O bond lengths

	Mn_3O_4		$CaMn_2O_4$*
Mn^{2+}-O(I)	2.6042(1) Å (2 ×)	Ca^{2+}-O(I)	2.646 Å (2 ×)
-O(II)	2.1248(16)	-O(II)	2.292
-O(II)	2.1479(16)	-O(II)	2.331
-O(III)	2.2690(11) (2 ×)	-O(III)	2.338 (2 ×)
-O(III)	2.3478(11) (2 ×)	-O(III)	2.468 (2 ×)
PV	22.00 Å		25.63 Å^3
Mn^{3+}-O(I)	2.3040(14) Å	Mn^{3+}-O(I)	2.478 Å
-O(I)	1.9469(12)	-O(I)	1.963
-O(II)	1.9159(3)	-O(II)	1.902
-O(III)	1.9252(11)	-O(III)	1.926
-O(III)	2.3222(12)	-O(III)	2.371
-O(III)	1.9143(4)	-O(III)	1.918
PV	11.34 Å^3		11.91 Å^3
QE	1.02106		1.03037
AV	18.892		17.937

Note: PV = polyhedral volume, QE = quadratic elongation, AV = angle variance.
* After Lepicard and Protas (1966).

References cited

Azároff, L.V. (1955) Polarization correction for crystal-monochromatized X-radiation. Acta Crystallographica, 8, 701–704.

Brown, I.D., and Altermatt, D. (1985) Bond-valence parameters obtained from a systematic analysis of the Inorganic Crystal Structure Database. Acta Crystallographica, B41, 244–247.

Flack, H.D., and Vincent, M.G. (1980) Testing for serial correlation in intensity data. Acta Crystallographica, A36, 495–496.

Hazen, R.M., and Finger, L.W. (1982) Comparative crystal chemistry, 231 p. Wiley, New York.

Hill, R.J., and Flack, H.D. (1987) The use of the Durbin-Watson *d* statistic in Rietveld analysis. Journal of Applied Crystallography, 20, 356–361.

Ito, E., Takahashi, E., and Matsui, Y. (1984) The mineralogy and chemistry of the lower mantle: An implication of the ultrahigh-pressure phase relations in the system MgO-FeO-SiO_2. Earth and Planetary Science Letters, 67, 238–248.

Jarosch, D. (1987) Crystal structure refinement and reflectance measurements of hausmannite, Mn_3O_4. Mineralogy and Petrology, 37, 15–23.

Lepicard, G., and Protas, J. (1966) Étude structurale de l'oxyde double de manganèse et de calcium orthorhombique $CaMn_2O_4$ (marokite). Bulletin de la Société Française de Minéralogie et de Cristallographie, 89, 318–324.

Liu, L.-G., and Bassett, W.A. (1986) Elements, oxides, silicates. High-pressure phases with implications for the Earth's interior, 250 p. Oxford University Press, New York.

Muller, O., and Roy, R. (1974) The major ternary structural families, 487 p. Springer-Verlag, New York.

Post, J.E., and Bish, D.L. (1988) Rietveld refinement of the todorokite structure. American Mineralogist, 73, 861–869.

Post, J.E., von Dreele, R.B., and Buseck, P.R. (1982) Symmetry and cation displacements in hollandites: Structure refinements of hollandite, cryptomelane and priderite. Acta Crystallographica, B38, 1056–1065.

Reid, A.F., and Ringwood, A.E. (1969) Newly observed high pressure transformations in Mn_3O_4, $CaAl_2O_4$, and $ZrSiO_4$. Earth and Planetary Science Letters, 6, 205–208.

Wiles, D.B., and Young, R.A. (1981) A new computer program for Rietveld analysis of X-ray powder diffraction patterns. Journal of Applied Crystallography, 14, 149–151.

Young, R.A., and Wiles, D.B. (1982) Profile shape functions in Rietveld refinements. Journal of Applied Crystallography, 15, 430–438.

Manuscript received February 28, 1990
Manuscript accepted October 1, 1990